Comparison of the viscoelastic properties of human abdominal and breast adipose tissue and its incidence on breast reconstruction surgery. A pilot study.

J.L. Calvo-Gallego[a,*], J. Domínguez[a], T. Gómez Cía[b], A. Ruiz-Moya[b], G. Gómez Ciriza[c], J. Martínez-Reina[a]

[a]*Department of Mechanical Engineering, University of Seville, Camino de los Descubrimientos s/n, Seville 41092, Spain*
[b]*Cirugía Plástica y Grandes Quemados, Hospital Virgen del Rocío, Seville, Spain*
[c]*Grupo de Innovación Tecnológica, Hospital Virgen del Rocío, Seville, Spain*

Abstract

This is a preprint of the paper, written before peer review. The reader is referred to the published version of this paper: https://doi.org/10.1016/j.clinbiomech.2019.10.009. Please, cite this work as: J.L. Calvo-Gallego, J. Domínguez, T. Gómez Cía, A. Ruiz-Moya, G. Gómez Ciriza and J. Martínez-Reina. Comparison of the viscoelastic properties of human abdominal and breast adipose tissue and its incidence on breast reconstruction surgery. A pilot study. Clinical Biomechanics. 2020; 71:37-44.

Background: breast cancer is the leading malignant tumour in women in the world. Reconstruction after mastectomy plays a key role in the physical and psychological recuperation, being the abdominal skin and adipose tissue the best current option for the DIEP surgery. The aim of the surgery is to obtain a reconstructed breast which looks and behaves naturally. Therefore, it would be useful to characterize the mechanical behavior of the adipose tissue in the abdomen and breast to compare their mechanical properties, also investigating possible regional differences.

Methods: experimental tests have been carried out in breast and abdominal adipose tissue samples, obtaining their viscoelastic properties. The specimens have been subjected to uniaxial compression relaxation tests and a mechanical behaviour model has been fitted to the experimental curves. Afterwards, statistical analyses have been used to detect differences between different individuals' abdominal fat tissue and finally between different areas of the same individual's breast and abdominal adipose tissue.

Findings: several conclusions could be extracted from the results: 1) inter-individual differences may exist in the abdominal adipose tissue; 2) the breast fat could be regarded as a unique tissue from the mechanical point of view; 3) significant differences were detected between the superficial breast and all the locations of the abdomen, except for the superficial lateral one and 4) the mechanical properties of the abdominal adipose tissue seem to change with the depth. These conclusions can be of great value for DIEP surgeries and other surgeries in which the adipose tissue is involved.

Keywords:

human adipose tissue, breast reconstruction, breast, abdomen, viscoelasticity

Abstract words: 247; Text words:4080; Annex words:525

1. Introduction

Breast reconstruction encompasses the restoration of the integrity, function and appearance of the breast mound after a partial/total resection, deformity or impairment caused by a disease, trauma, infection or whatever other agent. In our environment, the leading cause of breast absence/deformity is breast cancer [1].

Breast cancer is the most frequent malignant tumor in women worldwide [1]. With higher survival rates, more women are seeking breast reconstruction year after year. Reconstruction after mastectomy is of paramount importance for both the patient's physical and psychological recovery and well-being. Further than just restoring the physical integrity of the women's body and external appearance, it has been proved that it is also beneficial for their psychological recovery, psychosocial relationships and sexual activity [2, 3]. What is more important, women with reconstructed breasts show a better quality of life when compared with mastectomized non-reconstructed women [4].

It is crucial that the reconstructed breast looks, feels and behaves naturally to achieve the previous goals. In order to accomplish it, two main groups of reconstructive techniques exist: the autologous techniques, which use the patient's own tissue, and the alloplastic techniques, usually a two-stage procedure involving breast tissue expanders and prostheses (E-P). Autologous techniques offer the possibility of like-for-like tissue replacement, in contrast to alloplastic techniques.

The abdominal skin and fat tissue is nowadays considered as the optimal breast reconstructive technique by means of the deep inferior epigastric artery perforator (DIEP) flap [5, 6]. This flap has been adopted as the gold standard of autologous breast reconstruction, overtaking other popular autologous options such as the musculocutaneous latissimus dorsi flap and the transverse rectus abdominis miocutaneous (TRAM) flap. For example, it preserves and does not include muscle, contrarily to latissimus dorsi and TRAM flaps. The abdominal fat has a consistency, which is apparently similar to that of the breast, unlike other adipocutaneous flaps, as for example the gluteal flaps (SGAP/IGAP), which tend to be much firmer and fibrous. Besides, the abdominal skin thickness resembles that of the breast, in contrast to for example, the latissimus dorsi, with a much thicker skin that sometimes exhibits a patchy unnatural appearance in the reconstructed breast [6].

The DIEP technique shows several advantages: the amount of available tissue that allows for the reconstruction of both breasts if needed, the low abdominal morbidity for the patient, the ability of replacing like-for-like tissue and the

*Corresponding author. joselucalvo@us.es

good aesthetic results are the most notable, that have contributed to its widespread use [7]. The success rate of the procedure is high, with a flap loss rate under 3%, according to a review of more than 17.000 DIEP cases [8].

Although DIEP surgery is more expensive and needs a longer surgical time than E-P surgery, recent studies have showed that the former is cost-effective in comparison to the latter [9, 10]. Besides, patients reconstructed with DIEP flaps report a higher quality of life than patients reconstructed with prostheses in the short and in the long term [9]. On the other hand, E-P reconstructions often need a higher number of surgical procedures to achieve both the final result and contralateral symmetry, and regarding to the overall complication rate, it is also superior in this group, so as the surgeries derived from them [10]. In fact, when the long-term cost of these additional procedures is assessed, the E-P reconstruction becomes more expensive [10].

Although, it has been assured that the characteristics of the abdominal fat are the most similar to the breast tissue [6], this statement must be considered weak until the mechanical properties are directly and objectively compared, which has not been done yet in the literature, as far as the authors know.

The aim of this study is to present a method to characterize the mechanical behavior of the adipose tissue in several regions of the abdomen and breast, and also to investigate the regional differences across the abdomen. The hypothesis to be proven is that the viscoelastic properties of the abdominal fat are similar to those of the breast tissue for certain locations of the abdomen.

2. Methods

2.1. Test protocol

The experimental procedure was based on a previous work [11]. Next, a brief description of that procedure is given. However, the interested reader is referred to the original work for further details.

2.1.1. Preparation of specimens

The adipose tissue samples were extracted from the breast and the abdomen of two patients subjected to a mastectomy surgery. The abdominal tissue used in the experiments was the portion of the flap not eventually used for the reconstruction (see figure 1). The breast tissue (see figure 2) was obtained from the contralateral breast of one of the patients, who underwent a mastopexy to achieve the closest possible resemblance of both breasts.

Once excised, the pieces were introduced in a cool-box with dry ice to preserve them during transportation from the hospital to the mechanical engineering laboratory. The transport was done shortly after excision (as soon as possible) to minimize the time the tissue was at room temperature. In the lab, the skin was removed from the piece by cutting a slice of tissue of approximately 5 mm in depth (see Fig. 3). In the case of the abdominal fat, the rest of the piece was

Fig. 1: One of the pieces of abdominal fat from which specimens were extracted.

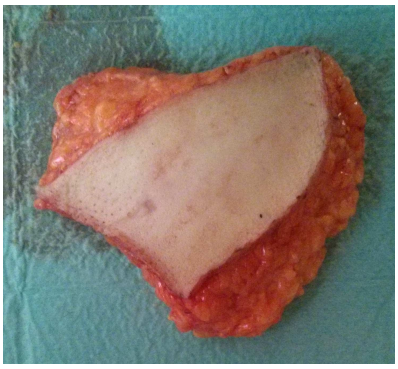

Fig. 2: Breast fat sample.

cut into two slices of approximately equal size: superficial, underneath the skin; and deep, on top of the abdominal muscle. Each slice was, in turn, cut into two parts (medial and lateral). The slices had a thickness ranging from 5 to 10 mm, which corresponded to the height of the tested specimens and was equal or smaller than the height of the specimens tested by Miller-Young et al. [12]. That height was limited to the mentioned range in order to avoid excessively slender specimens, which could lead to buckling problems. In the case of breast fat, only the division into superficial and deep parts could be done for size limitations. All these cuts were made with a meat slicer machine and a sharp knife. It was necessary to cut the slices while the tissue was still cool. The reason was that at room temperature the tissue is very soft and deformable, and the slices resulted in an unacceptable non-uniform thickness.

Due to the duration of the reconstruction surgery and the large number of specimens, it was not possible to test them all during the same day of extraction. Therefore, they were tested in the days that followed, as soon as possible to reduce the time elapsed from the excision to the test and freezing the tissue in the meantime to avoid its degradation. So, each slice of tissue was wrapped in saline-soaked gauze (saline solution: 0.9% w/v of NaCl), then in a plastic film, introduced in hermetic vials to prevent dehydration and finally frozen at $-20°C$.

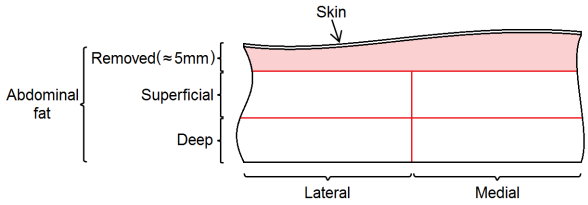

Fig. 3: Diagram of the divisions in the sample.

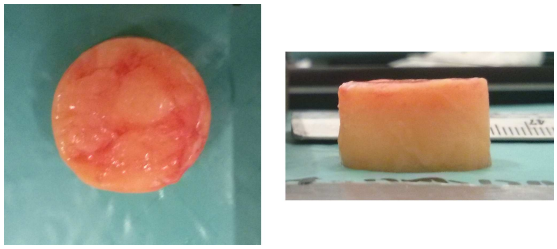

Fig. 4: Cylindrical specimen, top and lateral views.

Freezing of tissues may damage their microstructure under certain circumstances, compromising their structural integrity and altering the measured mechanical properties. The influence of freezing storage time at −20°C on the viscoelastic behaviour of the articular disc of the temporomandibular joint has been recently analyzed [13] to find that it has no effect if the storage time is shorter than one month. To the authors' knowledge, no similar study has been performed on adipose tissue, which could have a different sensitivity to freezing. However, the storage time is so much shorter in this case that no influence is expected.

The tests were carried out on cylindrical specimens, extracted from the slices with a hollow punch of 19mm in diameter. This extraction had to be done while the slice was frozen. Otherwise, the final shape of the specimens would be irregular and far from cylindrical, because the tissue would be largely deformed by the punch. A specimen with the final cylindrical shape can be seen in figure 4. Next, the specimen was submerged in saline solution at room temperature and allowed to thaw therein. Then, it was photographed to measure its area through imaging techniques.

2.1.2. Experimental setup

Uniaxial compression relaxation tests were carried out, compressing the cylindrical specimens between two metal platens. A servo-hydraulic testing machine (858 Mini Bionix II, MTS, Eden Prairie, USA) was used. A scheme of the experimental setup can be seen in figure 5.

Once the specimen was thawed, it was simply placed on the inferior platen, in the center. There was no need to glue it to the platen (in contrast to what occurred to other tissues [14]), because it remained within the platens in all the conducted tests. Next, the upper platen of the testing machine was brought into contact with the specimen's

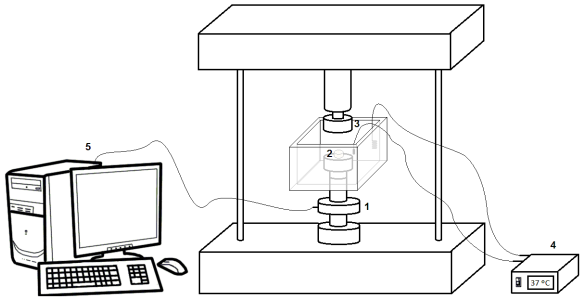

Fig. 5: Diagram of the test. Remarked: (1) loading cell, (2) sample, (3) upper platen, (4) temperature controller, (5) acquisition system.

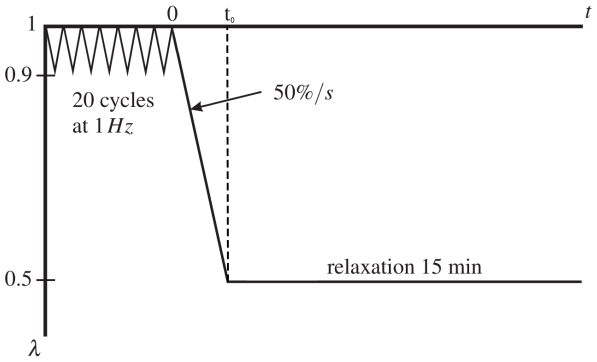

Fig. 6: Stretch (λ) vs. time in the relaxation test.

top surface and at this point the displacement was zeroed; that is, the distance between the platens defined the initial length of the specimen, L_0. The specimen remained submerged in saline solution at 37°C (range 36° − 38°C) during the whole test.

A preconditioning was applied to each sample: 20 cycles from 0% to 10% strain at 1 Hz, like in [15]. This was followed by a ramp from 0% to 50% strain as in [12, 16], and this final strain was maintained for 15 min, allowing for stress relaxation (see figure 6). This strain level corresponds to the breast compression reported by some authors [17, 18]. The strain rate of the loading ramp was 50% /s, as in [11]. During the test, the displacement of the upper platen, u, and the force exerted by it, F, were recorded. Finally, the stretch, λ, and Cauchy stress $\overline{\sigma}$, were respectively calculated using (A.7) (see Appendix).

The previous test is a modified version of the so called stress relaxation test. In an ideal stress relaxation test, the deformation (stretch) is applied as a step increase, but this leads to certain problems that make it unfeasible from a practical point of view. For that reason, the step increase was replaced by a ramp of finite strain rate, which only involves a different mathematical treatment of the results, discussed in [14].

2.2. Data fitting algorithm

The algorithm used here to fit the experimental results $\overline{\sigma} - \lambda$ was developed in a previous work [11] and is briefly explained in Appendix A. It is used to fit the parameters of a mathematical function that models the mechanical behaviour of adipose tissue. This mechanical behaviour is assumed viscoelastic, that is, the mechanical response of the material depends on the time elapsed since the application of the loads (visco) and the undeformed state is retrieved if the load is removed (elastic). In other words, there are neither plastic deformations nor damage.

The general response of viscoelastic materials to a stress relaxation test like that depicted in Fig. 6 is an immediate and abrupt increase in stress, which is relaxed with time, such that in the long term, as time tends to infinity, a certain stress lower than at the beginning, is required to keep the applied strain. The relation between that long-term stress and the strain is the long-term stiffness, associated to the elastic part, and the attenuation of stress, known as stress relaxation, is associated to the viscous part of the behaviour.

The constitutive model used here is an internal variable viscoelastic (IVV) model in which the elastic part is defined with a first order Ogden strain energy function, with two constants: μ and α. The viscous part is modelled with the superposition of exponentially decreasing functions (see Eq. (A.3)) and five constants: β_1^∞, β_2^∞, β_3^∞, β_4^∞ and β_5^∞. Each constant is associated with a given relaxation time, τ_i, which were chosen *a priori*. For example, $\tau_3 = 1\ s$ and $\tau_4 = 10\ s$. In this case β_3^∞ provides approximately the amount of stress relaxed from τ_3 to τ_4, that is, in the order of seconds.

Both sets of constants: elastic (μ and α) and viscous (β_i^∞) were fitted using the algorithm proposed in [11]. Then, they were compared between the different groups using a multivariable analysis of variance (MANOVA). Given that the stresses are not proportional to the model constants, their means are not representative statistics of the sample and the medians should be used instead. Thus, a non-parametric test (NMANOVA) is needed for the statistical comparison. The categorical independent variable (IV) had different levels that depend on the comparison and the dependent continuous variables (DVs) were the seven constants of the viscoelastic model (μ, α, β_i^∞, with $i = 1, 2, \ldots, 5$). The information about the patients and the samples is summarised in table 1.

2.2.1. Comparison between the abdominal fat for different patients

The objective of this comparison was to check the hypothesis that the mechanical properties of abdominal adipose tissue are different among individuals. For this purpose, the specimens extracted from patients A and B were compared (see table 1), pooling the anatomical locations. In other words, the IV was the patient with two levels: A and B. All the specimens were tested under the same conditions: strain level equal to 50% and strain rate equal to 50% /s.

Patient	Age	Extraction area	Location	Number of specimens
A	42	Abdomen	Superficial	8
			Deep	10
B	55	Abdomen	Superficial-lateral (ASL)	14
			Superficial-medial (ASM)	26
			Deep-lateral (ADL)	17
			Deep-medial (ADM)	23
		Breast	Superficial (BS)	12
			Deep (BD)	14

Table 1: Information of patients and tissue extracted.

2.2.2. Comparison between areas of the breast and abdominal fat in the same patient

The objective of this comparison was to check if the mechanical properties of different regions of the breast and abdominal adipose tissue are different for the same patient. For this purpose, the specimens extracted from patient B were used (see table 1). The IV was the anatomical location, with 6 levels: 1) abdominal superficial medial (ASM), 2) abdominal superficial lateral (ASL), 3) abdominal deep medial (ADM), 4) abdominal deep lateral (ADL), 5) breast superficial (BS) and 6) breast deep (BD). All the specimens were tested under the same conditions: strain level equal to 50% and strain rate equal to 50% /s.

3. Results

Figure 7 compares a typical experimental stress record ($\tilde{\sigma}$ vs. time) with the fitting curve.
As in [11], the raw stress record, $\overline{\sigma}$, was filtered to remove the signal noise, by using a moving average filter. The resulting stress record, named $\tilde{\sigma}$, was fitted to the analytical stress record, σ, using a least squares method, that minimizes the following quadratic error:

$$e = \sum_{i=1}^{N} \left(\tilde{\sigma}(t_i) - \sigma(t_i)\right)^2 \tag{1}$$

where N is the total number of points recorded during the relaxation test and t_i is the instant of a certain point. The goodness of the least squares fit was evaluated by means of the coefficient of variation, CV:

$$CV(\%) = \frac{\sqrt{\frac{e}{N}}}{\mu_{\tilde{\sigma}}} \times 100 \tag{2}$$

where $\mu_{\tilde{\sigma}}$ is the average of the temporal record $\tilde{\sigma}(t_i)$. The obtention of the experimental and analytical stresses ($\overline{\sigma}$ and

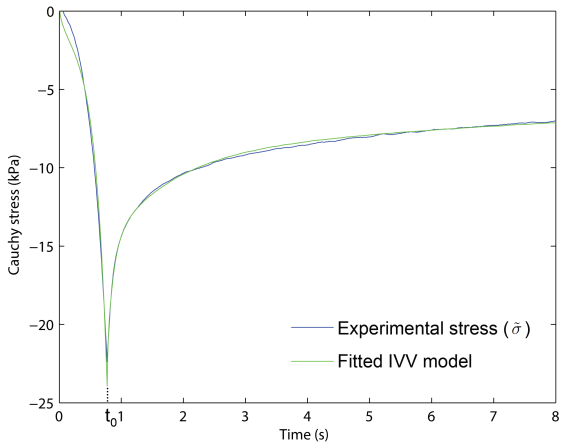

Fig. 7: Example of a experimental stress record and the fitting curve using the proposed model.

Patient	Extraction area	Whole curve CV (%)	Loading ramp CV (%)
A	Abdomen	3.86	16.39
B	Abdomen	4.05	14.23
	Breast	3.17	10.47

Table 2: Coefficient of variation for each patient and region.

σ, respectively) is briefly explained in the Appendix.

The average CV for each patient and model are presented in table 2. The CV was separately evaluated for the whole curve and for the loading ramp (from $t = 0$ to $t = t_0$, see figures 6 and 7).

The only work found in the literature that measured experimentally the mechanical properties of breast fat is that of Samani and Plewes [19]. These authors carried out pseudostatic indentation tests to estimate the elastic properties of the tissue using a five-terms polynomial hyperelastic model. Those results are compared in Fig. 8 with the long-term stiffness (associated to the elastic part) of the present model. More precisely, that figure compares the stress-stretch curves that both models would produce in the simulation of a pseudostatic tension-compression uniaxial test. As can be seen, the differences between both curves are quite noticeable, even for small stretches, being the Samani and Plewes's model much stiffer than the one fitted here. This can be due to the fact that Samani and Plewes performed their tests under a finite strain rate (2% /s), but they did not consider the viscous effect, which makes the response of the material stiffer than in pseudostatic conditions.

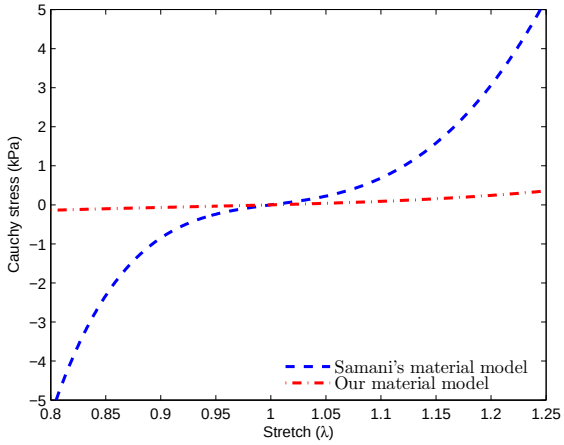

Fig. 8: Comparison between Samani and Plewes's model and the one fitted here for the breast adipose tissue.

3.1. Comparison between the abdominal fat for different individuals

A NMANOVA was carried out to search for differences between the samples extracted from both individuals. The categorical IV had 2 levels: abdominal fat of patient A and abdominal fat of patient B; and the dependent variables were the seven constants of the IVV model: μ, α and β_i^{∞}, with $i = 1, 2, \ldots, 5$.

The NMANOVA test performed in this work was a multivariate extension of the Kruskal-Wallis test, developed by Katz and McSweeney [20]. Significant differences were found between the samples of both patients ($p = .002$). Next, the Katz and McSweeney's post-hoc test [20] was carried out to detect the origin of the differences between patients A and B. Significant differences were found for μ ($p = 0.002$), β_4^{∞} ($p = 0.013$) and β_5^{∞} ($p = 0.004$). Multivariate analyses of variance are indicated if the dependent variables are correlated, but not so strongly that multicollinearity exists. In this case β_4^{∞} and β_5^{∞} were strongly correlated (Spearman $R = .83$). Therefore, β_5^{∞} was removed from the set of DVs and the analysis was repeated considering the remaining 6 DVs. The conclusion was the same: significant statistical differences were found in the omnibus test ($p = .001$) with significant differences in the post hoc test of the same variables: μ ($p < 0.001$) and β_4^{∞} ($p = 0.011$).

In table 3, the median and interquartile range of the material constants are given for each patient.

3.2. Comparison between areas of the breast and abdominal fat

To check the regional dependence of the material constants of the abdominal and breast fat, a NMANOVA test was used. Given that the mechanical properties can be subject specific as deduced from the previous comparison, the regional dependence was checked for a single individual. The independent variable was the anatomical location

Patient	Quartile	μ (kPa)	α	β_1^∞	β_2^∞	β_3^∞	β_4^∞	β_5^∞
A	Q1	0.079	6.583	57.331	10.312	3.774	1.786	1.721
	Median	0.109	7.595	95.788	13.253	4.214	2.177	2.187
	Q3	0.137	9.301	147.593	16.479	4.874	2.494	2.473
B	Q1	0.042	7.701	71.132	10.888	3.161	1.440	1.406
	Median	0.057	8.513	91.459	15.045	3.737	1.687	1.633
	Q3	0.076	9.584	132.245	18.753	4.520	2.060	1.958

Table 3: Median and interquartile range for the constants of the IVV model for the abdominal adipose tissue, for patients A and B.

	BS	BD	ASL	ASM	ADL	ADM
BS		$p = .111$	$p = 1$	$\mathbf{p = .001}$	$\mathbf{p = .004}$	$\mathbf{p < .001}$
BD			$p = 1$	$p = 1$	$p = 1$	$p = 1$
ASL				$p = .069$	$\mathbf{p = .032}$	$\mathbf{p = .015}$
ASM					$\mathbf{p = .032}$	$p = .192$
ADL						$p = 1$
ADM						

Table 4: Post-hoc comparisons, showing the lowest p-value of the seven dependent variables in each cell and highlighting in bold typeface the significant ones ($p < .05$).

with six levels: ASM, ASL, ADM, ADL, BS, BD, and the DVs were the seven material constants: μ, α, β_i^∞, with $i = 1, 2, \ldots, 5$.

Significant differences were found between the six groups using the Katz and McSweeney's test ($p < .001$). The Katz and McSweeney's post-hoc tests were carried out to detect the origin of these differences. Significant differences were found for the following constants: β_2^∞ (between BS and ASM, $p = .001$, and between ADL and ASM, $p = .003$); β_3^∞ (between BS and ASM, $p = .006$); β_4^∞ (between BS and ADM, $p = .002$; between BS and ADL, $p = .004$; between BS and ASM, $p = .042$; between the ADM and ADL, $p = .015$; and between ADL and ASL, $p = .032$) and β_5^∞ (between BS and ADM , $p < .001$, and between BS and ADL, $p = .013$).

In this case, β_3^∞, β_4^∞ and β_5^∞ were strongly correlated (Spearman $R > .82$) and could be regarded as the same variable from a statistical point of view. Therefore the test was repeated considering only β_4^∞ from these three variables, to check the correctness of the previous conclusion. Again, significant differences were found in the omnibus test ($p < .001$). The p-values of the post-hoc comparisons are summarized in table 4, showing the lowest p-value of the seven dependent variables in each cell and highlighting in bold typeface the significant ones ($p < .05$). Many p-values are equal to one because the Bonferroni correction was used for the comparisons. All the values that were higher than one due to this correction were set equal to one.

In summary, there are differences between the mechanical properties of the superficial breast and three groups of the

abdomen: superficial-medial, deep-medial and deep-lateral. In contrast, the differences with the superficial lateral and with the deep layer of the breast fat are not significant. No significant differences were detected between the deep breast and the rest of the groups either.

The differences in the mechanical properties are illustrated in Fig. 9, which compares the stress relaxation response simulated using the medians shown in table 5 for BS and ADM. It can be seen that the viscoelastic behaviour is quite different, but as time tends to infinity, the curves tend to merge into one, viz. the long-term elastic behaviour (once the viscous effect is damped) is similar in both groups. The same can be said in other comparisons. In fact, no significant differences were observed in μ or α.

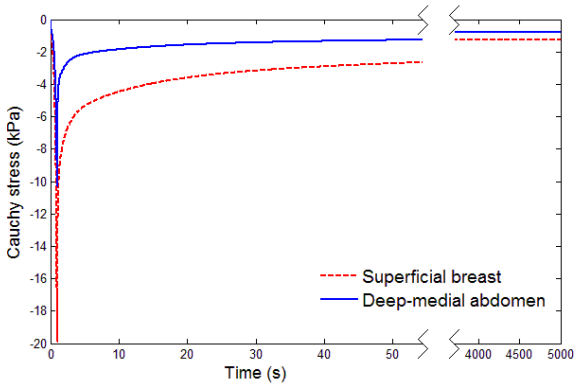

Fig. 9: Comparison between the stress relaxation response simulated using the median constants of superficial breast and deep-medial abdomen.

In table 5, the median and interquartile range of the material constants of each anatomical location are presented.

Area	Quartile	μ (kPa)	α	β_1^∞	β_2^∞	β_3^∞	β_4^∞	β_5^∞
BS	Q1	0.041	8.311	37.919	17.583	4.497	2.793	2.485
	Median	0.058	8.875	67.286	20.520	5.584	3.160	2.824
	Q3	0.080	10.069	101.902	25.603	7.773	4.890	3.467
BD	Q1	0.043	7.402	57.948	10.754	3.068	1.321	1.252
	Median	0.057	7.949	65.934	16.891	3.446	1.861	1.623
	Q3	0.092	9.058	100.745	18.867	4.469	2.190	2.091
ASL	Q1	0.042	7.869	52.950	13.135	4.143	2.316	1.948
	Median	0.060	8.552	74.568	14.208	4.983	2.636	2.387
	Q3	0.109	9.888	89.457	19.230	6.111	3.331	2.556
ADL	Q1	0.042	7.125	81.435	14.961	2.883	1.182	1.379
	Median	0.057	8.220	114.741	18.180	3.866	1.542	1.629
	Q3	0.069	9.018	192.804	22.936	4.845	1.875	1.803
ASM	Q1	0.042	7.747	77.993	8.881	2.921	1.471	1.540
	Median	0.058	8.862	91.459	10.783	3.504	1.664	1.627
	Q3	0.099	10.026	123.956	13.879	3.770	2.003	1.905
ADM	Q1	0.038	7.534	71.524	13.219	3.368	1.366	1.357
	Median	0.048	8.099	103.708	17.091	3.734	1.613	1.483
	Q3	0.066	9.175	148.504	19.762	4.274	1.801	1.797

Table 5: Median and interquartile range for constants of the IVV model for the different abdominal and breast areas of patient B.

4. Discussion

As can be seen in figure 7 and deduced from the CVs of table 2, the fit of the IVV model is quite accurate, as presented in a previous study of the abdominal adipose tissue [11].

The model fitted in this work resulted much more flexible than that previously obtained by Samani and Plewes [19]. This may be due to the fact that those authors performed cyclic loading at a finite strain rate and assumed the tissue as elastic, instead of viscoelastic, thus neglecting the stiffening effect of the viscous response.

In view of the results of the statistical analysis in section 3.1, inter-individual differences were suspected both in the elastic and viscous constants. For this reason, it seemed appropriate to use only the specimens of one individual for the comparison of the anatomical region.

Regarding the comparison between the mechanical properties of the different regions of breast and abdominal fat, the breast adipose tissue could be regarded as a unique tissue from the mechanical point of view. Significant differences were detected between the superficial breast and three groups in the abdomen. However, no significant differences were found between the breast and the superficial-lateral abdomen. Significant differences were not found between the deep breast and the rest of the groups.

It is interesting to remark that all the differences were detected in the viscous constants, which control the stress

relaxation rate. Apparently, the elastic constants were similar for the whole adipose tissue, both of the breast or the abdomen. Thus, the behaviour under static loading could be considered equivalent. This conclusion has a high relevance for the breast reconstruction surgery, because the deformed shape of the breast would not be affected by using autologous tissue from the abdomen, at least in situations when the load is static or pseudostatic. That would not be the case of dynamic loading, like impacts or bouncing for example, and in these cases the reconstructed breast could respond in a different manner.

In view of the results obtained here, if the whole behaviour, including the dynamic one, is to be mimicked, the deep breast fat could be replaced by any part of the abdomen and the superficial breast fat should be replaced by the superficial lateral region. However, autologous breast reconstructions are usually made of a single piece of abdominal fat tissue. For that reason, the most advisable protocol would be using a flap extracted from the superficial lateral area of the abdomen. Nevertheless, it must be taken into account that the lateral areas of the abdomen are the least reliable from a vascular point of view in DIEP reconstruction. Hartrampfs' zone IV is almost invariably discarded for its tendency towards congestion and necrosis, while in zone III dermal bleeding must be always assessed to ensure optimal irrigation and to avoid skin and/or fat necrosis [8, 21]. Otherwise, it is advised to partially or totally discard it as well.

Also important, although with less clinical relevance, are the significant differences found between the regions of the abdominal adipose tissue. The results of the present work show no significant differences between the mechanical properties of both parts of the superficial layer (medial and lateral), between both parts of the deep layer (medial and lateral) and between both parts of the medial regions (superficial and deep). However, significant differences were found between the deep and superficial layers. That is to say, the mechanical properties of the abdominal adipose tissue seem to change with the depth. This fact is in accordance with other authors [22], who suggested that, though they could not prove it.

As a pilot study, the main limitation of the present study is the number of individuals involved in it. The variability of the properties across individuals was checked only in two patients and the variability across anatomical regions in one patient. In the latter case, the number of tested specimens is enough to support the statistical conclusion for that patient, because the differences were very significant, but these conclusions need to be confirmed in further studies which involve more patients.

5. Conclusions

In this work, the viscoelastic properties of the breast and abdominal adipose tissue have been determined through experimental tests. The specimens have been subjected to uniaxial compression relaxation tests and an IVV model

has been fitted to the experimental curves, obtaining a quite accurate fit.

Statistical analyses of the results have been carried out to detect differences between the abdominal fat of different individuals and finally between several regions of the same individual: different areas of the breast and abdominal adipose tissue. The results showed that: 1) inter-individual differences may exist in the abdominal adipose tissue; 2) the breast fat could be regarded as a unique tissue from the mechanical point of view; 3) differences were detected between the superficial breast and three groups in the abdomen and 4) the mechanical properties of the abdominal adipose tissue seem to change with the depth.

It is important to say that all the differences were detected in the stress relaxation constants, that is to say, the elastic constants were similar for the whole adipose tissue for the same patient.

These conclusions can be very valuable for many surgeries in which the adipose tissue is involved. For instance, in the breast reconstruction surgeries with autologous tissue in which the breast is reconstructed with abdominal fat and whose aim is to mimic the deformed shape of the healthy breast.

Conflict of interest statement

The authors declare that they have no conflict of interest.

Acknowledgements

The authors gratefully acknowledge the research support from the 'Ministerio de Economía y Competitividad de España' through the research project DPI2011-28080, 'Modelado numérico de un proceso de reconstrucción mamaria'.

References

References

[1] International Agency for Research on Cancer. Globocan 2012: Estimated cancer incidence, mortality and prevalence worldwide 2012.

[2] Alderman AK, Wilkins EG, Lowery JC, et al. Determinants of patient satisfaction in postmastectomy breast reconstruction. *Plastic and Reconstructive Surgery* 2000; **106**:769–776.

[3] Guyomard V, Leinster S, Wilkinson M. Systematic review of studies of patients' satisfaction with breast reconstruction after mastectomy. *Breast* 2007; **16(6)**:547–567.

[4] Eltahir Y, Werners LL, Dreise MM, et al. Quality-of-life outcomes between mastectomy alone and breast reconstruction: comparison of patient-reported breast-q and other health-related quality-of-life measures. *Plastic and Reconstructive Surgery* 2013; **132**:201–209.

[5] Allen RJ, Treece P. Deep inferior epigastric perforator flap for breast reconstruction. *Annals of Plastic Surgery* 1994; **32**:32–38.

[6] Grotting JC. *Plastic and Reconstructive Surgery 3rd Edition*, vol. 5. Saunders, 2013.

[7] Zhong T, McCarthy C, Min S, et al. Patient satisfaction and health-related quality of life after autologous tissue breast reconstruction: a prospective analysis of early postoperative outcomes. *Cancer* 2012; **118**:1701–1709.

[8] Lie KH, Barker AS, Ashton MW. A classification system for partial and complete diep flap necrosis based on a review of 17.096 diep flaps in 693 articles including analysis of 152 total flap failures. *Plastic and Reconstructive Surgery* 2013; **132**:1401–1408.

[9] Matros E, Albornoz CR, Razdan SN, et al. Cost-effectiveness analysis of implants versus autologous perforator flaps using the breast-q. *Plastic and Reconstructive Surgery* 2015; **135**:937–946.

[10] Lagares-Borrego A, Gacto-Sanchez P, Infante-Cossio P, et al. A comparison of long-term cost and clinical outcomes between the two-stage sequence expander/prosthesis and autologous deep inferior epigastric flap methods for breast reconstruction in a public hospital. *Journal of Plastic, Reconstructive and Aesthetic Surgery* 2016; **69**:196–205.

[11] Calvo-Gallego JL, Domínguez J, Gómez-Cía T, et al. Comparison of different constitutive models to characterize the viscoelastic properties of human abdominal adipose tissue. a pilot study. *Journal of the Mechanical Behavior of Biomedical Materials* 2018; **80**:293–302.

[12] Miller-Young JE, Duncan NA, Baroud G. Material properties of the human calcaneal fat pad in compression: experiment and theory. *Journal of Biomechanics* 2002; **35**:1523–1531.

[13] Calvo-Gallego JL, Commisso MS, Domínguez J, et al. Effect of freezing storage time on the elastic and viscous properties of the porcine tmj disc. *Journal of the Mechanical Behaviour of Biomedical Materials* 2017; **71**:314–319.

[14] Commisso MS, Martínez-Reina J, Mayo J, et al. Numerical simulation of a relaxation test designed to fit a quasi-linear viscoelastic model for temporomandibular joint discs. *Proceedings of the Institution of Mechanical Engineers, Part H: Journal of Engineering in Medicine* 2013; **227 (2)**:190–199.

[15] Allen KD, Athanasiou KA. Viscoelastic characterization of the porcine temporomandibular joint disc under unconfined compression. *Journal of Biomechanics* 2006; **39**(5):312–322.

[16] Commisso MS, Calvo-Gallego JL, Mayo J, et al. Quasi-linear viscoelastic model of the articular disc of the temporomandibular joint. *Experimental Mechanics* 2016; **56(7)**:1169–1177.

[17] Ruiter N, Stotzka R, Muller T, et al. Model-based registration of X-ray mammograms and MR images of the female breast. *IEEE transactions on nuclear science* 2006; **53**:204–211.

[18] Han L, Hipwell JH, Tanner C, et al. Development of patient-specific biomechanical models for predicting large breast deformation. *Physics in Medicine and Biology* 2012; **57**:455–472.

[19] Samani A, Plewes D. A method to measure the hyperelastic parameters of ex vivo breast tissue samples. *Physics in Medicine and Biology* 2004; **49**:4395–4405.

[20] Katz BM, McSweeney M. A multivariate Kruskal-Wallis test with post-hoc procedures. *Multivariate Behavioral Research* 1980; **15**:281–297.

[21] Bailey SH, Saint-Cyr M, Wong C, et al. The single dominant medial row perforator diep flap in breast reconstruction: Three- dimensional perforasome and clinical results. *Plastic and Reconstructive Surgery* 2010; **126**:739–751.

[22] Sommer G, Eder M, Kovacs L, et al. Multiaxial mechanical properties and constitutive modeling of human adipose tissue: a basis for preoperative simulations in plastic and reconstructive surgery. *Acta Biomaterialia* 2013; **9 (11)**:9036–9048.

[23] Holzapfel GA. *Nonlinear solid mechanics: A continuum approach for engineering*. Wiley: Chichester, England, 2000.

[24] Holzapfel GA, Gasser TC. A viscoelastic model for fiber-reinforced composites at finite strains: continuum basis, computational aspects and applications. *Computer Methods in Applied Mechanics and Engineering* 2001; **190**:4379–4403.

[25] Lanczos C. *Applied Analysis*. Prentice-Hall: New Jersey, 1956.

[26] Troyer KL, Estep DJ, Puttlitz CM. Viscoelastic effects during loading play an integral role in soft tissue mechanics. *Acta Biomaterialia* 2012; **8**:234–243.

[27] Holzapfel GA, Gasser TC, Ogden RW. A new constitutive framework for arterial wall mechanics and a comparative study of materials models. *Journal of Elasticity* 2000; **61**:1–48.

Appendix A. Data fitting algorithm

The viscoelastic model used in the present paper was proposed in a previous work [11] and is briefly presented in this appendix for those readers interested in the mathematical details. It is an internal variable viscoelastic (IVV) model which implements a first order Ogden strain energy function for the elastic response. Many authors have used this IVV model [23], or its extension to fiber models presented in [24], to characterize the mechanical behaviour of different materials. The interested reader is referred to the previous work [11], where the experimental procedure was explained in more detail. In this IVV model, the second Piola-Kirchhoff stress tensor takes the form:

$$\mathbf{S} = \mathbf{S}^{\infty}_{\text{vol}} + \mathbf{S}^{\infty}_{\text{iso}} + \sum_{i=1}^{m} \mathbf{Q}_i \tag{A.1}$$

with $\mathbf{S}^{\infty}_{\text{vol}}$ and $\mathbf{S}^{\infty}_{\text{iso}}$ the fully elastic volumetric and isochoric contributions to the second Piola-Kirchhoff stress tensor respectively, and $\mathbf{Q}_i$ representing the non-equilibrium stresses, or internal variables. The evolution equations of the latter are:

$$\dot{\mathbf{Q}}_i + \frac{\mathbf{Q}_i}{\tau_i} = \dot{\mathbf{S}}_{\text{iso}\,i} \tag{A.2}$$

where τ_i and $\mathbf{S}_{\text{iso}\,i}$ are the relaxation time and the isochoric second Piola-Kirchhoff stress tensor, respectively. The solution of the differential equation (A.2) for $t \in (0, T]$ is:

$$\mathbf{Q}_i = e^{-T/\tau_i}\,\mathbf{Q}_{i\,0^+} + \int_{t=0^+}^{t=T} e^{-(T-t)/\tau_i}\ \dot{\mathbf{S}}_{\text{iso}\,i}(t)\,dt \tag{A.3}$$

where $\mathbf{Q}_{i\,0^+}$ is the stress initial condition, viz. the instantaneous stress tensor appearing at $t = 0^+$. The following assumption is made to define the strain energy function, $\Psi_{\text{iso}\,i}$:

$$\Psi_{\text{iso}\,i}(\bar{\mathbf{C}}) = \beta_i^{\infty}\Psi^{\infty}_{\text{iso}}(\bar{\mathbf{C}}) \tag{A.4}$$

$\Psi^{\infty}_{\text{iso}}$ is the isochoric stain energy function as time tends to infinity, $\bar{\mathbf{C}} = \bar{\mathbf{F}}^T\bar{\mathbf{F}}$ is the modified right Cauchy-Green tensor, $\bar{\mathbf{F}} = J^{-1/3}\mathbf{F}$ is the modified deformation gradient tensor, with $\mathbf{F}$ the deformation gradient tensor and J the volume ratio. With the assumption (A.4), the stress $\mathbf{S}_{\text{iso}\,i}$ can be simplified as:

$$\mathbf{S}_{\text{iso}\,i} = \beta_i^{\infty}\mathbf{S}^{\infty}_{\text{iso}}(\bar{\mathbf{C}}) \tag{A.5}$$

The constants β_i^{∞} are dimensionless strain energy factors. For the non-equilibrium forces $\mathbf{Q}_i$, 5 terms were selected as

in [11], viz. $i = 1, 2, \ldots, 5$, being each term responsible for the relaxation of stresses in specified intervals. To do this, the relaxation time constants, τ_i, were fixed *a priori*, which also ensured the uniqueness of the fitted set of constants [25, 26]. In particular, they were taken in decades: $\tau_1 = 0.01\ s$, $\tau_2 = 0.1\ s$, $\tau_3 = 1\ s$, $\tau_4 = 10\ s$ and $\tau_5 = 100\ s$ [11].

A first order Ogden formulation was chosen for the strain energy function:

$$\Psi_{\text{iso}}^{\infty} = \frac{\mu}{\alpha}(\lambda_1^{\alpha} + \lambda_2^{\alpha} + \lambda_3^{\alpha} - 3) \tag{A.6}$$

since this was the best fitting function for the adipose tissue, as presented in [11]. In equation (A.6), μ is a stress-like parameter, α a dimensionless parameter and λ_j ($j = 1, 2, 3$) are the principal stretches.

The preconditioning cycles were not considered in the fitting algorithm. So, time was zeroed after those cycles (see figure 6). Knowing the stretch history $\lambda = \lambda(t)$ from $t = 0$ onwards, $\mathbf{S}_{\text{vol}}^{\infty}$ and $\mathbf{S}_{\text{iso}}^{\infty}$ can be derived for uniaxial compression from (A.6), by following classical procedures of Continuum Mechanics [23].

Then, $\mathbf{S}_{\text{iso}}^{\infty}$ is used in (A.5) and (A.3) to calculate $\mathbf{Q}_i$ and equation (A.1) is used to give $\mathbf{S}$. Finally, the Cauchy stress tensor was obtained using the well known relation $\boldsymbol{\sigma} = J^{-1}\mathbf{F}\mathbf{S}\mathbf{F}^T$, whose component in the load direction is the stress σ in Eq. (1). The algorithm proposed in [27] was followed to implement these equations. Consulting that reference is advised for further details.

The experimental Cauchy stress was estimated from the applied force, F, recorded during the test, by assuming uniaxial compression:

$$\overline{\sigma}(t) = \frac{F(t)\ \lambda(t)}{A_0}, \qquad \lambda(t) = 1 + \frac{u(t)}{L} \tag{A.7}$$

where A_0 is the initial cross-sectional area of the sample, $u(t)$ is the displacement of the upper platen, and L is the initial thickness of the specimen.